Therapeutics, Targets, and Chemical Biology

Cancer Research

EGFRvIII Antibody–Conjugated Iron Oxide Nanoparticles for Magnetic Resonance Imaging–Guided Convection-Enhanced Delivery and Targeted Therapy of Glioblastoma

Costas G. Hadjipanayis[1], Revaz Machaidze[1], Milota Kaluzova[1], Liya Wang[2], Albert J. Schuette[1], Hongwei Chen[2], Xinying Wu[2,3], and Hui Mao[2]

Abstract

The magnetic nanoparticle has emerged as a potential multifunctional clinical tool that can provide cancer cell detection by magnetic resonance imaging (MRI) contrast enhancement as well as targeted cancer cell therapy. A major barrier in the use of nanotechnology for brain tumor applications is the difficulty in delivering nanoparticles to intracranial tumors. Iron oxide nanoparticles (IONP; 10 nm in core size) conjugated to a purified antibody that selectively binds to the epidermal growth factor receptor (EGFR) deletion mutant (EGFRvIII) present on human glioblastoma multiforme (GBM) cells were used for therapeutic targeting and MRI contrast enhancement of experimental glioblastoma, both *in vitro* and *in vivo*, after convection-enhanced delivery (CED). A significant decrease in glioblastoma cell survival was observed after nanoparticle treatment and no toxicity was observed with treatment of human astrocytes ($P < 0.001$). Lower EGFR phosphorylation was found in glioblastoma cells after EGFRvIIIAb-IONP treatment. Apoptosis was determined to be the mode of cell death after treatment of GBM cells and glioblastoma stem cell–containing neurospheres with EGFRvIIIAb-IONPs. MRI-guided CED of EGFRvIIIAb-IONPs allowed for the initial distribution of magnetic nanoparticles within or adjacent to intracranial human xenograft tumors and continued dispersion days later. A significant increase in animal survival was found after CED of magnetic nanoparticles ($P < 0.01$) in mice implanted with highly tumorigenic glioblastoma xenografts (U87ΔEGFRvIII). IONPs conjugated to an antibody specific to the EGFRvIII deletion mutant constitutively expressed by human glioblastoma tumors can provide selective MRI contrast enhancement of tumor cells and targeted therapy of infiltrative glioblastoma cells after CED. *Cancer Res; 70(15); 6303–12. ©2010 AACR.*

Introduction

Despite the use of conventional therapeutic modalities such as surgery, chemotherapy, and ionizing radiation, the prognosis in patients with malignant gliomas remains poor (1). Virtually all glioblastoma multiforme (GBM) tumors, the most common malignant glioma, recur at the site of their initial treatment due to the presence of infiltrating cancer cells in the surrounding normal brain that resist therapy or go untreated. Infiltrating cancer cells include a subpopulation of glioblastoma stem cells (GSC) shown to be integral to tumor development, perpetuation, and therapy resistance (2, 3). Imaging and targeted therapy of infiltrating GBM cells within the normal brain remain limited.

The epidermal growth factor receptor variant III (EGFRvIII) is a tumor-specific mutation that is expressed in malignant gliomas and not in the normal brain. This mutation encodes a constitutively active tyrosine kinase that enhances tumorigenicity and accounts for radiation and chemotherapy resistance (4, 5). The 801-bp in-frame deletion in the extracellular domain of the EGFR results in the fusion of normally distant *EGFR* gene and protein sequences (6, 7). The 14-amino-acid fusion junction sequence has been chemically synthesized and used to create an anti–synthetic peptide antibody that is highly specific for the deletion mutant EGFR protein compared with the intact EGFR protein (8, 9). Vaccination of the fusion junction peptide sequence has been shown to be efficacious immunotherapy in syngeneic murine models and in humans with two consecutive and one multi-institutional phase II trials (10).

The magnetic nanoparticle has emerged as a potential multifunctional clinical tool that can provide cancer cell detection by magnetic resonance imaging (MRI) contrast enhancement as well as therapy by cancer cell–targeted delivery of therapeutic agents (antibodies, drugs, and small-molecule inhibitors)

Authors' Affiliations: [1]Brain Tumor Nanotechnology Laboratory, Department of Neurosurgery and [2]Department of Radiology, Winship Cancer Institute, Emory University School of Medicine, Atlanta, Georgia; and [3]Department of Radiology, Zhejiang University School of Medicine, Hangzhou, Zhejiang Province, P.R. China

Note: Supplementary data for this article are available at Cancer Research Online (http://cancerres.aacrjournals.org/).

Corresponding Author: Costas G. Hadjipanayis, Department of Neurosurgery, Emory University School of Medicine, 1365B Clifton Road Northeast, Suite 6200, Atlanta, GA 30322. Phone: 404-778-3091; Fax: 404-778-4472; E-mail: chadjip@emory.edu.

doi: 10.1158/0008-5472.CAN-10-1022

or by local hyperthermia generated by absorbing energy from an alternating magnetic field. Iron oxide nanoparticles (IONP) in the size range of 10 to 25 nm have unique magnetic properties, generating significant transverse T_2 relaxation time shortening and susceptibility effects resulting in strong T_2-weighted contrast on MRI (11). IONPs can evade the immune system and target cancer cells for destruction while simultaneously providing MRI contrast. Most IONPs are biodegradable and considered to have low toxicity (12). IONPs have been used in the clinical setting with humans (13). Currently, various formulations of IONPs have been developed for drug delivery schemes (14), magnetic cell separation and cell targeting (15), magnetic resonance imaging (MRI) contrast enhancement (16–20), and hyperthermia treatment of cancer (17, 21–23).

Cell-specific imaging by nanotechnology for detection and treatment monitoring holds great promise for the therapy of various cancers including central nervous system (CNS) tumors (24, 25). However, a major barrier in the use of nanotechnology for brain tumor applications is the difficulty in delivering nanoparticles to intracranial tumors. Conventional systemic delivery is limited due to the nonspecific nanoparticle uptake by the reticuloendothelial system and problems in penetrating the blood-brain barrier (BBB). Convection-enhanced delivery (CED) is a minimally invasive surgical procedure that provides fluid convection in the brain by a pressure gradient that bypasses the BBB. Therapeutic agents can be delivered into the brain by CED in high concentrations (26, 27) without toxicity to normal tissue and organs commonly associated with systemic delivery. The use of CED can also allow for therapeutic targeting of infiltrating cancer cells, a major cause for brain tumor recurrence after surgery. We report the use of IONPs conjugated to an anti–synthetic peptide antibody (EGFRvIIIAb) specific to the deletion-mutant EGFR for image-guided CED in a mouse glioma model. The EGFRvIIIAb-IONP complex can provide MRI contrast enhancement of human glioblastoma cells *in vitro* and an antitumor effect both *in vitro* and *in vivo* after CED.

Materials and Methods

Animals, cells, and EGFRvIII antibody

The human glioblastoma cell line U87MG was obtained from the American Type Culture Collection within the last 6 months and maintained in standard culture conditions. The U87MG cell line was stably transfected with either a plasmid for overexpression of the deletion mutant EGFRvIII (U87ΔEGFRvIII) or the wild-type (wt) EGFR (U87wtEGFR) and tested by Western blot analysis (Supplementary Fig. S1). Neurospheres were harvested from patient GBM specimens (patients #74, 1002, and 30) at the time of surgical resection and cultured using serum-free medium supplemented with growth factors. Patient tumor specimens were harvested with approval by the Emory University Institutional Review Board (protocol #642-2005). Glioblastoma neurospheres were tested by Western blot analysis (Supplementary Fig. S2) for the GSC stem cell marker CD133 (Cell Signaling), EGFRvIII (GenScript Corp.), and wt EGFR (Cell Signaling). Overexpression of the deletion mutant EGFRvIII confers enhanced tumorigenicity in immunocompromised rodents (4). Six- to seven-week-old athymic nude (nu/nu) mice were used, and all procedures were done with approval by the Institutional Animal Care and Use Committee of Emory University. The IgG polyclonal EGFRvIII antibody (6 nm and 150 kDa) was generated by GenScript in rabbits and purified as described in a prior publication (8). Briefly, the rabbit polyclonal EGFRvIIIAb represents an anti–synthetic peptide antibody that reacts to the fusion junction of the deletion mutant EGFRvIII receptor expressed in human glioblastoma tumors.

IONP bioconjugation

Briefly, activation of the carboxyl groups on the IONPs was performed for conjugation of the EGFRvIII antibody, after addition of an activation buffer, ethyl dimethylaminopropyl carbodiimide (EDC), and sulfo-NHS. The EDC/NHS solution was mixed vigorously with the IONPs at 25°C for 15 minutes. Excess EDC and sulfo-NHS were removed from the activated nanoparticles by three rounds of centrifugation (1,000 × *g*) and resuspension in PBS using Nanosep 10K MWCO OMEGA membrane (Pall Life Sciences). The IONPs with activated carboxyl groups were then reacted with the EGFRvIII antibody (50 μL at 2 mg/mL) at 25°C for 2 hours, and the reaction mixture was stored at 4°C overnight. Excess antibody was removed by three rounds of centrifugation and resuspension in PBS using 300K MWCO OMEGA membranes. Mobility shift in 1% agarose gel was visualized by staining with 0.25% Coomassie brilliant blue in 45% methanol, 10% acetic acid for 1 hours and destaining in 30% methanol, 10% acetic acid overnight (Supplementary Fig. S3).

Binding of IONPs to glioblastoma cells

Glioblastoma cells (U87ΔEGFRvIII) were seeded in triplicate in 60-mm flat-bottomed plates and incubated overnight at 37°C. Confluent monolayers of cells (1×10^6) were incubated with the IONP or EGFRvIIIAb-IONP solution (0.15 mg/mL) for 1 or 2 hours for MRI experiments. Washing of cells was performed with 10% PBS to remove the excess nanoparticle solution. Treated cells were collected after scraping and placed in 10-mL tubes containing warm 0.8% agarose solution. MRI measurements were made with a 3-T clinical capable scanner. The T_2 relaxation times of cells treated with IONPs were measured using a multi-echo fast spin echo sequence with 32 TE values ranging from 6 to 180 ms and an interval of 6 ms. The T_2 relaxation time was calculated by fitting the decay curve using the nonlinear monoexponential algorithm of $M_{(TE)} = M_0 \times \exp(-TE/T_2)$. See Supplementary Methods for transmission electron microscopy (TEM) studies.

Human astrocyte and glioblastoma cell IONP toxicity studies

Human astrocytes were kindly provided by the Yong Laboratory at the University of Calgary, Alberta, Canada. The astrocytes were cultured based on a prior published protocol (28). Toxicity experiments were performed on human astrocytes seeded in triplicate in 48-well flat-bottomed plates (10^5 astrocytes per well). Cells were treated with free IONPs (0.3 mg/mL)

or control vehicle (serum-free medium) for 1 hour at 37°C. Glioblastoma cells (U87MG and U87ΔEGFRvIII) were seeded in triplicate in 48-well flat-bottomed plates (80,000 cells per well) and incubated overnight at 37°C. Confluent monolayers of cells were washed with PBS and then incubated with control (PBS), IONPs (0.2 mg/mL), EGFRvIIIAb (0.2 mg/mL), or EGFRvIIIAb-IONPs (0.2 mg/mL) for 1 hour at 37°C. Cells were then washed with PBS and a crystal violet cell viability assay was performed at 0, 1, and 3 days. Cells were stained with 100 μL of crystal violet solution (1% crystal violet, 1% HCl, and 10% ethanol) at 37°C for 30 minutes. Absorbance measurements were performed on a microtiter plate reader at a wavelength of 570 nm. Absorbance values are presented as the mean of three wells per treatment ± SD.

Glioblastoma apoptosis and EGFR cellular signaling studies after IONP treatment

Glioblastoma cells (U87MG, U87ΔEGFRvIII, and U87wtEGFR) and neurospheres from patients #30 and 74 were seeded in six-well flat-bottomed plates (500,000 cells per well) and incubated overnight at 37°C. Cells were treated with control IgG (0.3 mg/mL), IONPs (0.3 mg/mL), EGFRvIIIAb (0.3 mg/mL), and EGFRvIIIAb-IONPs (0.3 mg/mL) for 2 to 3 hours in PBS at 37°C. Cells were lysed in radioimmunoprecipitation assay (RIPA) buffer [50 mmol/L Tris (pH 8.0), 150 mmol/L NaCl, 5 mmol/L EDTA, and 1% NP40, with protease and phosphatase inhibitors]. Western blot analysis of protein levels was performed with cleaved caspase-3 and caspase-3 primary antibodies (Cell Signaling) according to the manufacturer's recommendations.

For EGFR signaling studies, glioblastoma cells were treated with control (PBS), IONPs (0.5 mg/mL), EGFRvIIIAb (0.5 mg/mL), and EGFRvIIIAb-IONPs (0.5 mg/mL) for 2 hours in PBS at room temperature. Cell lysates were harvested in RIPA buffer [50 mmol/L Tris (pH 8.0), 150 mmol/L NaCl, 5 mmol/L EDTA, and 1% NP40, with protease and phosphatase inhibitors]. Western blot analysis of protein levels was performed with primary antibodies against phospho-EGFR (Transduction Laboratories), phosho-Akt (Cell Signaling), Akt (Cell Signaling), phospho-extracellular signal–regulated kinase (ERK)-44/42 (Cell Signaling), and ERK44/42 (Cell Signaling) according to the manufacturer's recommendations. Horseradish peroxidase (HRP)–conjugated secondary antibodies (Dako) and a chemoluminescent HRP detection solution (Denville Scientific, Inc.) were used to detect the proteins.

Tumor inoculation and IONP convection procedure

Anesthetized athymic nude mice were placed in the stereotaxic instrument and U87ΔEGFRvIII cells (5×10^5) were stereotactically inoculated into the right striatum, 3 mm below the dural surface, on day 0. On day 7 after tumor implantation, mice were randomized into four groups: (*a*) CED of HBSS (untreated control), (*b*) CED of IONPs, (*c*) CED of EGFRvIIIAb, and (*d*) CED of EGFRvIIIAb-IONPs. All animals underwent CED of a 10-μL volume at a rate of 0.5 μL/min (20 minutes of total infusion) on day 7 using the same coordinates as used earlier for tumor cell implantation. For the CED methods, see Supplementary Methods.

The volume of distribution and volume of dispersion of IONPs after CED

Mice inoculated with U87ΔEGFRvIII cells (5×10^5) were also followed by MRI to investigate the initial volume of distribution (V_D) and volume of dispersion (V_{DI}) of IONPs over a period of 11 days after CED. Animals underwent CED of IONPs (n = 3 free IONPs and n = 3 EGFRvIIIAb-IONPs) as described above on day 9 after tumor implantation. These animals were scanned on a 4.7-T animal MRI scanner using a dedicated mouse coil (Varian Unity) on days 0, 4, 7, and 11 after CED. The V_D was determined for each animal (n = 4) on days 0, 4, 7, and 11 after CED. The V_{DI} of the IONPs on days 4, 7, and 11 was determined by subtracting the V_D at day 0 from the V_D calculations on days 4, 7, and 11 after CED of the IONPs (e.g., V_{DI} day 4 = V_D day 4 − V_D day 0). For V_D and V_{DI} measurements, see Supplementary Methods.

Histology

Mouse brains were harvested and fixed with 10% neutral buffered formalin on days 7 and 9 after tumor implantation. Coronal sections were made at the level of the needle tract to mark the center of the xenograft tumor. Serial sections of the cerebral hemisphere were examined from each animal. Tissue blocks were embedded in paraffin and sectioned (5 μm). Prussian blue staining was performed after slides of formalin-fixed tissue were placed in a coplin jar containing a 1:1 mixture of 5% potassium ferrocyanide and 5% HCl for 30 minutes at 37°C in a water bath. The slides were rinsed well with distilled water and counterstained with nuclear fast red for 20 minutes (Supplementary Fig. S4). EGFRvIII immunohistochemistry was performed (day 7 after tumor implantation) after deparaffinization of tissue sections (Supplementary Fig. S5). The primary rabbit polyclonal EGFRvIII antibody (GenScript) and a biotinylated antirabbit secondary antibody provided in a rabbit ABC staining system (Santa Cruz Biotechnology) were used.

Animal survival studies

All athymic nude mice were observed daily to monitor external appearance, feeding behavior, and locomotion. Animals were sacrificed at the first sign of an adverse event (paresis, inability to feed) and brains were removed.

Statistical analysis

Cell viability data represent the average of three independent absorbance values on day 3 of the crystal violet assay. Statistical cell viability differences were assessed using unpaired two-sample Student's t test assuming equal variance. Animal survival data were entered into Kaplan-Meier plots and statistical analysis was performed using log-rank test. P = 0.05 was considered statistically significant.

Results

EGFRvIIIAb-IONP bioconjugate

Amphiphilic triblock copolymer–coated IONPs (10 nm in size; provided by Ocean Nanotech, LLC) were covalently conjugated to a purified rabbit polyclonal EGFRvIIIAb (Supplementary Fig. S1). The IONP surface coating provides a stable

hydrophobic protective inner layer around a single crystal of IONP with carboxylate groups in the outer layer for functionalization (29). Bioconjugation was performed with the amino-terminal fragment of the antibody and carboxyl groups on the copolymer coating of the IONPs (Fig. 1). Confirmation of the antibody conjugation to IONPs was performed by agarose gel electrophoresis analysis (Supplementary Fig. S3).

Confirmation of binding of EGFRvIIIAb-IONPs to human glioblastoma cells by MRI and TEM

The binding affinity of EGFRvIIIAb-IONPs to human GBM cells that overexpress the EGFRvIII mutated protein was evaluated. The EGFRvIIIAb-IONP conjugate was able to selectively bind to U87ΔEGFRvIII cells and induce T_2-weighted MRI contrast enhancement after 1 and 2 hours of treatment (Fig. 2; Table 1), as evidenced by the MRI signal drop compared with the control samples of cells treated with free IONPs. Such strong T_2 shortening and the magnetic susceptibility effects of IONPs lead to spin dephasing and substantial MRI signal drop, which generated a "darkening" contrast as seen in the T_2-weighted MR images. TEM confirmed binding of EGFRvIIIAb-IONPs to the cell surface of EGFRvIII-expressing glioblastoma cells as shown in Supplementary Fig. S6. No evidence of endocytosis and endosome-filled EGFRvIIIAb-IONPs was found in glioblastoma cells based on TEM. In contrast, treatment of cells with free IONPs revealed nonspecific cell surface binding, uptake, and IONP-filled endosomes within the cytoplasm of U87ΔEGFRvIII cells (Supplementary Fig. S7).

IONPs exhibit no toxicity to human astrocytes

To determine whether IONPs are toxic to human astrocytes, cells were treated with control vehicle (serum-free medium) or IONPs (0.3 mg/mL) for 1 hour. After cell washing, a crystal violet cell viability assay was performed. There was no significant toxicity found with human astrocytes 3 days after treatment with IONPs ($P < 0.001$; Fig. 3A).

Antitumor effect of IONPs on human glioblastoma cells

Human glioblastoma cells (U87-MG or U87ΔEGFRvIII) were incubated with control (PBS), EGFRvIIIAb, IONPs, or EGFRvIIIAb-IONPs for 1 hour (Fig. 3B and C). Cells were washed and cell viability assay was performed at 0, 1, and 3 days after treatment. At day 3, there was a significant decrease in cell survival in U87ΔEGFRvIII cells treated with IONPs, EGFRvIIIAb, or EGFRvIIIAb-IONPs ($P < 0.001$). There was a less pronounced but statistically significant decrease in cell survival in U87MG cells treated with IONPs, EGFRvIIIAb, or EGFRvIIIAb-IONPs ($P < 0.01$). Nonspecific uptake of free IONPs likely accounts for cell toxicity and the antitumor effect found in both glioblastoma cell lines (Supplementary Fig. S7).

Apoptosis as a mode of cell death of GBM cell– and GSC-containing neurospheres after EGFRvIIIAb-IONP treatment

Human glioblastoma cells (U87MG, U87ΔEGFRvIII, and U87wtEGFR) and neurospheres were incubated with control IgG, EGFRvIIIAb, IONPs, and EGFRvIIIAb-IONPs (Fig. 4). Western blot analysis revealed elevated levels of cleaved caspase-3 in glioblastoma cells (Fig. 4A) and neurospheres (Fig. 4B) treated with EGFRvIIIAb-IONPs. No levels of cleaved caspase-3 were found with treatment of glioblastoma cells with free IONPs, control IgG, or EGFRvIIIAb. Elevated levels of cleaved caspase-3 and apoptosis were found in human glioblastoma neurospheres harvested from patients #30 and 74 after treatment with the EGFRvIIIAb-IONPs

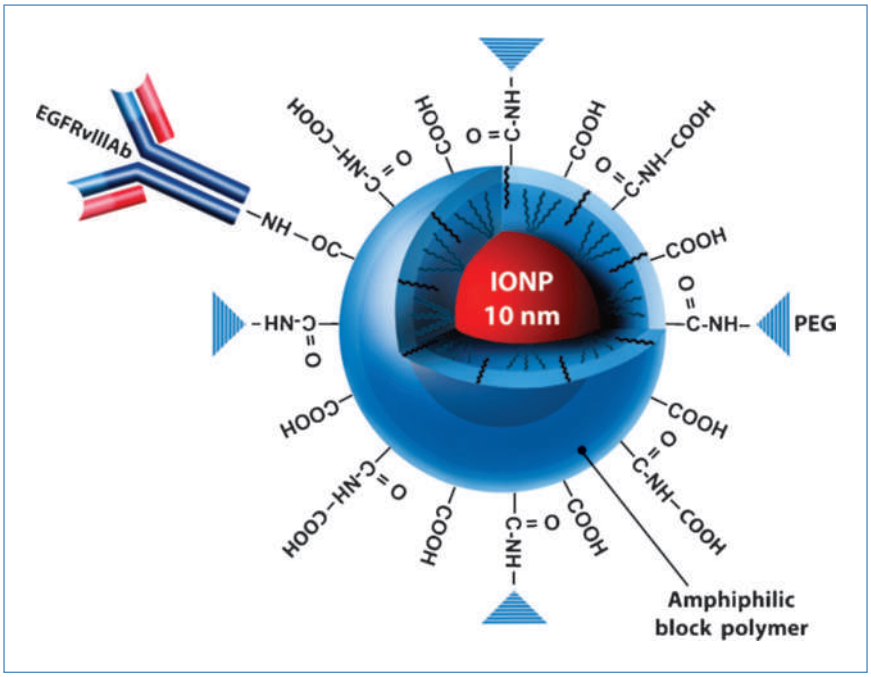

Figure 1. Amphiphilic block polymer–coated IONPs conjugated to the EGFRvIIIAb. Illustration of IONP (shown in red; core size of 10 nm) coated with a biocompatible amphiphilic copolymer bioconjugated to the EGFRvIIIAb (illustration provided by Eric Jablonowski, Department of Radiology, Emory University School of Medicine). Polyethylene glycols (PEG) are present on the surface of the polymer for further stabilization and biocompatibility of the IONP. Bioconjugation of the EGFRvIII antibody is performed to the -COOH of the polymer coating of the IONP.

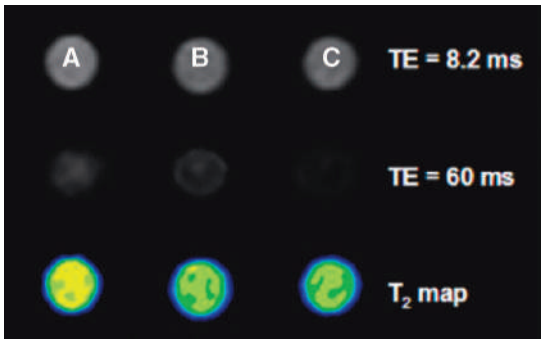

Figure 2. Binding of EGFRvIIIAb-IONPs to human glioblastoma cells and MRI contrast enhancement. The binding of EGFRvIIIAb-conjugated IONPs to human GBM cells that overexpress the EGFRvIII mutated protein was confirmed by MRI contrast changes (lower signal intensity at longer TE in T_2-weighted imaging and reduction of T_2 values as shown in Table 1B and C after 1 and 2 h of treatment) when compared with the control samples of free IONPs (A).

(Fig. 4B). Glioblastoma neurospheres from patient #30 are characterized by EGFRvIII, wt EGFR, and CD133 GSC marker expression, whereas neurospheres from patient #74 express wt EGFR (Supplementary Fig. S2).

Glioblastoma EGFR signaling and IONPs

Ligand activation of the EGFR leads to a series of downstream signaling events after phosphorylation and activation (30, 31). Western blot analysis of EGFR cellular signaling proteins was performed in glioblastoma cells (U87MG, U87wtEGFR, and U87ΔEGFRvIII) treated with control (PBS), IONPs, EGFRvIIIAb, or EGFRvIIIAb-IONPs (Fig. 4C). Levels of phosphorylated EGFR, phospho-Akt, Akt, ERK44/42, and phospho-ERK44/42 were determined. Both U87wtEGFR and U87ΔEGFRvIII showed elevated levels of phosphorylated EGFR as expected due to the overexpression of EGFR in these cell lines. U87ΔEGFRvIII cells showed the greatest EGFR phosphorylation due to the constitutive activity of the EGFRvIII receptor. Treatment of these cells with EGFRvIIIAb-IONPs showed a lower level of EGFR phosphorylation. Treatment of U87wtEGFR and U87ΔEGFRvIII glioblastoma cells with either IONPs or EGFRvIIIAb-IONPs resulted in less phosphorylation of Akt and no phosphorylation of ERK, suggesting that IONPs may affect downstream EGFR signaling in glioblastoma cells. Treatment of U87wtEGFR and U87ΔEGFRvIII glioblastoma cells with EGFRvIIIAb alone resulted in increase in phosphorylated Akt and ERK levels.

CED of EGFRvIIIAb-IONPs in a mouse glioma model

Athymic nude mice (n = 6) implanted with human GBM xenografts that express the mutated EGFRvIII protein (U87ΔEGFRvIII) underwent CED of EGFRvIIIAb-IONPs (n = 3) or IONPs (n = 3) in aqueous solution (0.2 mg/mL concentration; 10 μL volume; 0.5 μL/min rate for a total of 20 minutes) 9 days after tumor implantation. MRI was performed before CED to confirm proper growth of the xenograft in each mouse brain (Fig. 5) and then 0, 4, 7, and 11 days after CED of the nanoparticles to determine localization, initial V_D, and V_{DI} of the IONPs administered (Fig. 5). Average V_D values were 11.2, 19.2, 22.7, and 22.9 mm^3 on days 0, 4, 7, and 11, respectively. The averaged V_{DI} values were 8.0, 11.5, 15.5 mm^3 on days 4, 7, and 11 after CED. There was no statistically significant difference in the V_D and V_{DI} of free IONPs and EGFRvIIIAb-IONPs. Prussian blue staining was performed to confirm the presence of EGFRvIIIAb-IONPs in human xenograft tumors and the surrounding mouse brain after CED (Supplementary Fig. S4).

Several initial findings support the feasibility of the MRI-guided CED of IONPs in human xenograft brain tumors: (*a*) EGFRvIIIAb-IONPs can be distributed within or adjacent to brain tumors with CED; (*b*) outstanding contrast induced by IONPs enables MRI to monitor and follow the distribution of the nanoparticle complex in the tumor and in the surrounding brain after CED; (*c*) intracerebral infusion is safe, as all animals survived from the procedures and showed no signs of toxicity; (*d*) CED led to a long retention of the EGFRvIIIAb-conjugated nanoparticles and slow dispersion of the agents at the tumor site as shown on MRI; (*e*) MRI can delineate and quantify the extent of dispersion of the IONP complex after CED with T_2-weighted MRI.

Animal survival studies and therapeutic efficacy of EGFRvIIIAb-IONPs after CED

Animal survival studies were performed in four groups of mice implanted with highly tumorigenic U87ΔEGFRvIII xenografts (Fig. 6; Supplementary Fig. S5). Each group of animals (n = 10) underwent CED of control (HBSS), unconjugated IONPs (0.2 mg/mL), EGFRvIIIAb (0.2 mg/mL), or EGFRvIIIAb-IONPs (0.2 mg/mL) 7 days after tumor implantation. All the animals that underwent HBSS CED were dead by 14 days after tumor implantation (median survival, 11 days).

Table 1. MRI T_2 values after treatment of U87ΔEGFRvIII cells with free IONPs or EGFRvIIIAb-IONPs

	Sample	T_2 (cal.) s^{-1}
A	U87ΔEGFRvIII cells + IONPs 2 h	0.053
B	U87ΔEGFRvIII cells + EGFRvIIIAb-IONPs 1 h	0.037
C	U87ΔEGFRvIII cells + EGFRvIIIAb-IONPs 2 h	0.026

NOTE: A, cells were treated with free IONPs for 1 h. B and C, a reduction in T_2 values (MRI contrast enhancement) was found after glioblastoma cells were treated for 1 and 2 h with EGFRvIIIAb-IONPs.

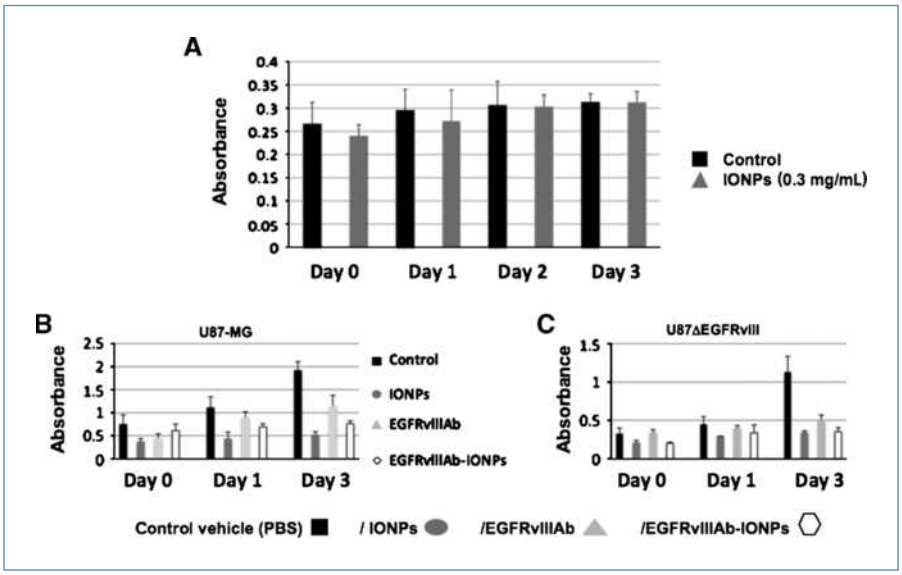

Figure 3. Cell toxicity analysis of human astrocytes and glioblastoma cells treated with IONPs. A, human astrocytes were treated with control vehicle (serum-free medium) or IONPs at 0, 1, 2, and 3 d. No significant toxicity was found with IONP treatment in human astrocytes ($P < 0.001$). Cell toxicity analysis of human glioblastoma cells [U87-MG (B) and U87ΔEGFRvIII (C)] after treatment with control vehicle (PBS), IONPs, EGFRvIIIAb, and EGFRvIIIAb-IONPs at 0, 1, and 3 d. A significant decrease in cell survival was found in glioblastoma cells treated with IONPs, EGFRvIIIAb, and EGFRvIIIAb-IONPs on day 3 ($P < 0.001$).

A significant increase in survival was found in animals that underwent CED of IONPs (median survival, 16 days), EGFRvIIIAb (median survival, 17 days), and EGFRvIIIAb-IONPs (median survival, 19 days) compared with animals that underwent CED of HBSS ($P < 0.001$). Both the EGFRvIIIAb and EGFRvIIIAb-IONP treatment groups have a single survivor after 120 days of survival studies.

Discussion

Accurate targeting and better delivery efficiency are two major goals in the development of therapeutic agents for the treatment of malignant brain tumors. Ideally, a therapeutic agent would be able to overcome the BBB and selectively be enriched in tumors with minimal toxicity to

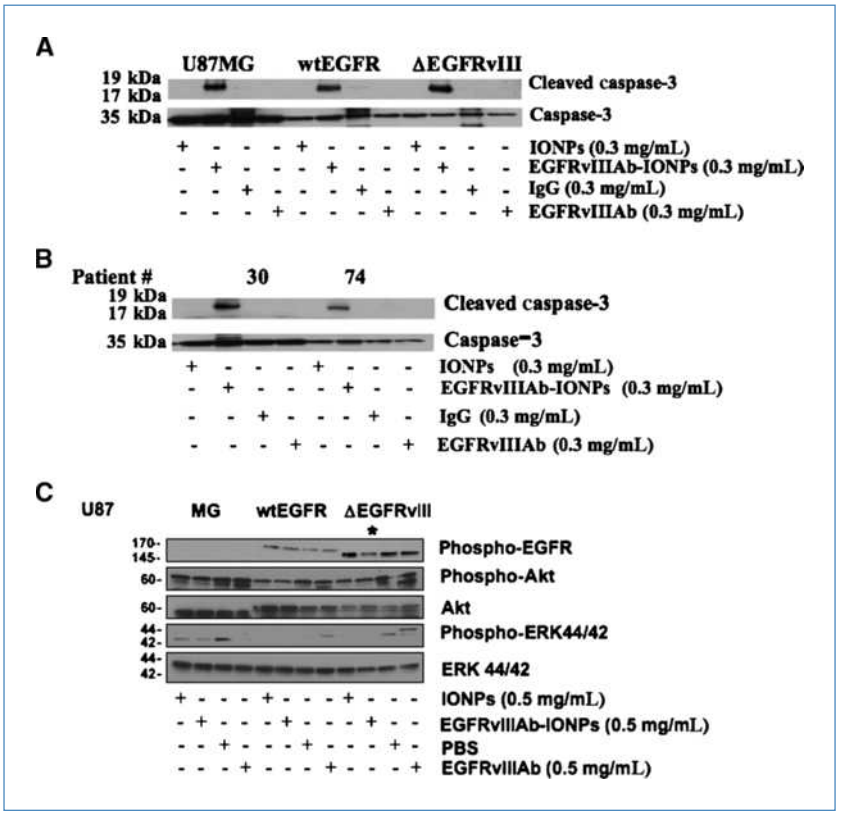

Figure 4. Apoptosis studies and glioblastoma EGFR cellular signaling after treatment with EGFRvIIIAb-IONPs. A, elevated levels of cleaved caspase-3 and apoptosis were found in all human glioblastoma cells (U87MG, U87ΔEGFRvIII, and U87wtEGFR) after treatment with EGFRvIIIAb-IONPs. B, elevated levels of cleaved caspase-3 and apoptosis were found in human glioblastoma neurospheres harvested from patients #74 and 30 after treatment with EGFRvIIIAb-IONPs. C, glioblastoma EGFR cellular signaling after treatment with IONPs, EGFRvIIIAb-IONPs, control vehicle (PBS), and EGFRvIIIAb. Western blot analysis of glioblastoma cells (U87MG, U87wtEGFR, and U87ΔEGFRvIII) reveals lower level of the phosphorylated and active form of EGFR (*) in U87ΔEGFRvIII cells after treatment with EGFRvIIIAb-IONPs.

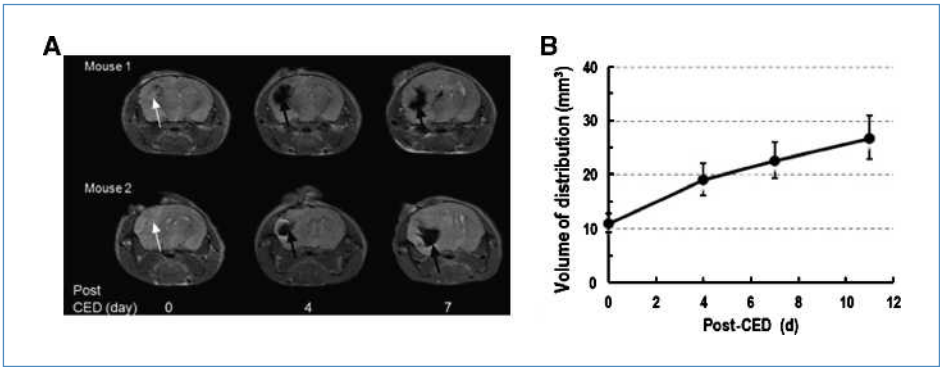

Figure 5. CED of EGFRvIIIAb-IONPs in a mouse glioma model. A, examples of T_2-weighted images of mouse brains (mouse 1 and mouse 2) show the presence of intracranial xenograft (shown by white arrows) and reveal the localization, distribution, and dispersion of magnetic nanoparticles at days 4 and 7 after CED (shown by black arrows). T_2-weighted MRI shows a decrease in signal after CED of IONPs. Areas with signal drop increased 7 d after CED, showing dispersion of nanoparticles. B, initial nanoparticle V_D after CED is shown at day 0. The V_{DI} was determined at 4, 7, and 11 d after CED, confirming dispersion of nanoparticles.

normal tissues. Conjugation of agents to antibodies or other ligands that bind to antigens or receptors that are usually abundantly or uniquely expressed on the tumor surface represents a promising approach in the treatment of glioblastoma tumors (32, 33). Unfortunately, the ability to image therapeutic agents in the brain for adequate tumor delivery and the proper assessment of treatment efficacy remain limited.

The use of nanotechnology is now being applied to CNS cancer applications (13, 25, 34–39). One potential problem that can attenuate the targeted therapy and imaging of CNS tumors by systemic delivery of nanoparticles is their being "trapped" in the liver, spleen, and circulating macrophages after i.v. administration due to nonspecific uptake. Additionally, systemic delivery is also limited by the BBB, nontargeted distribution, and systemic toxicity. CED is an approach developed to overcome the obstacles associated with current CNS agent delivery (26, 27, 40) and is increasingly used to distribute therapeutic agents for treatment of malignant gliomas (27). Recently, multiple clinical trials

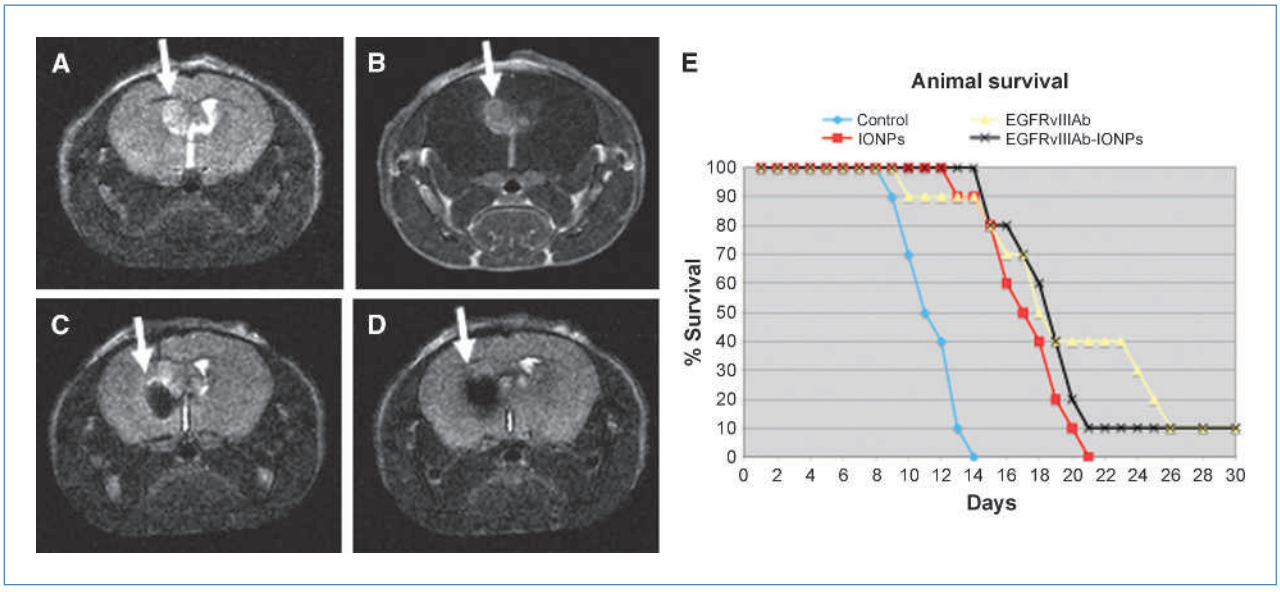

Figure 6. Survival studies of athymic nude mice implanted with human U87ΔEGFRvIII xenografts after magnetic nanoparticle CED. A, T_2-weighted MRI showing a tumor xenograft with bright signal 7 d after tumor implantation (arrow); B, tumor shown (arrow) by contrast enhancement after injection of gadolinium contrast agent (Gd-DTPA); C, MRI signal drop (arrow) after CED of EGFRvIIIAb-IONPs; D, EGFRvIIIAb-IONP dispersion and T_2 signal drop (arrow) on MRI 4 d after CED. E, Kaplan-Meier survival curve comparison of athymic nude mice after intracranial implantation of human U87ΔEGFRvIII cells and treatment by MRI-guided CED of HBSS (control), IONPs, EGFRvIIIAb, or EGFRvIIIAb-IONPs. Statistical significance ($P < 0.001$) was estimated by log-rank method of CED of EGFRvIIIAb-IONPs, IONPs, and EGFRvIIIAb compared with HBSS CED.

have been performed using CED for the treatment of recurrent GBM (32, 33, 41). In CED, a small hydrostatic pressure differential imposed by a syringe pump to distribute infusate directly to small or large regions of the CNS is used in a safe, reliable, targeted, and homogeneous manner (42). Difficulty in CED imaging of therapeutic agents in the brain is one major limitation of this approach. Groups have radiolabeled their therapeutic agent, co-infused their agent with radiolabeled albumin (^{123}I-labeled albumin), or used liposomes containing an MRI contrast agent (e.g., gadoteridol) for CED imaging (33, 43, 44). Radiolabeling of therapeutic agents relies on single-photon emission computerized tomography for agent imaging, which is a low-resolution imaging modality of the brain. Co-infusion of an MRI contrast agent or radiolabeled albumin may not allow for precise therapeutic agent distribution analysis in the brain due to the differences in molecular weight and surface properties between each infusate. Recently, CED of biodegradable, nonfunctionalized maghemite magnetic nanoparticles has been depicted by MRI in a normal rat brain model (45). Direct imaging of magnetic nanoparticles by MRI can permit distribution studies of nanoparticles in the brain after CED.

Currently, two major types of systemic anti-EGFR agents have entered the clinical setting: anti-EGFR antibodies and small-molecule EGFR tyrosine kinase inhibitors (46–48). These agents have shown modest efficacy in patients with GBM tumors. The development of new agents that can target the EGFR deletion mutant EGFRvIII can permit direct targeting of glioblastoma cells while sparing the normal brain (9, 49–52). Furthermore, the targeting of GSCs and/or GSC-specific molecules (e.g., CD133) may form the basis of more effective treatments against glioblastoma tumors and prevention of relapse (2).

We report for the first time the use of IONPs bioconjugated to an EGFRvIII deletion mutant antibody for MRI-assisted CED and targeted therapy of human glioblastoma. The bioconjugated EGFRvIIIAb-IONPs permit MRI contrast enhancement or "darkening" of U87ΔEGFRvIII cells with T_2-weighted MRI. The EGFRvIIIAb-IONPs caused a significant decrease in glioblastoma cell survival, and a greater antitumor effect was found after treatment of EGFRvIII-expressing glioblastoma cells with EGFRvIIIAb-IONPs in comparison with human glioblastoma cells, which did not express the EGFR. This provided further evidence of a biomarker-targeting effect by the EGFRvIIIAb-IONPs. The pronounced antitumor effect of free IONPs in glioblastoma cells is likely due to the nonspecific uptake of the nanoparticles by the tumor cells. Uptake of IONPs by glioma cells has been shown in culture and *in vivo* in the past (53, 54). The influence of surface functionalization has recently been shown to enhance the internalization of magnetic nanoparticles in cancer cells (55). Our IONPs are functionalized through surface coating of amphiphilic polymers, which may promote uptake within glioblastoma cells and result in cell toxicity.

No significant toxicity was found with IONP treatment in human astrocytes or in animals after intracerebral administration. No toxicity to human astrocytes and a significant killing effect of both free IONPs and EGFRvIIIAb-IONPs form the basis of targeted therapy of GBM cells in the brain. Apoptosis was determined to be a mode of cell death after treatment of glioblastoma cells and neurospheres by the conjugate EGFRvIIIAb-IONP. Apoptosis was found after treatment of GSC-containing neurospheres harvested from a glioblastoma patient (patient #30) with elevated expression of EGFRvIII and the GSC marker CD133. Although we were not able to find apoptosis induction in glioblastoma cells after treatment with free IONPs or the EGFRvIIIAb alone, a significant antitumor effect was found both *in vitro* and in our animal survival studies. Mechanistic studies suggest that EGFR downstream signaling may be affected by IONPs with less EGFR phosphorylation after glioblastoma cell treatment with EGFRvIIIAb-IONPs. Furthermore, IONPs resulted in less phosphorylation of Akt and ERK in glioblastoma cells overexpressing the EGFR.

CED of IONPs in a mouse glioma model results in MRI contrast of the nanoparticles and effective intratumoral and peritumoral distribution of nanoparticles in the brain. A significant therapeutic effect was found after CED of both IONPs and EGFRvIIIAb-IONPs in mice. Dispersion of the nanoparticles over days, after the infusion has finished, may potentially target infiltrating tumor cells outside the tumor mass that are potentially responsible for tumor recurrence and the demise of patients. Use of bioconjugated magnetic nanoparticles may permit the advancement of CED in the treatment of malignant gliomas due to their sensitive imaging qualities on standard T_2-weighted MRI and therapeutic effects. Better targeting of infiltrative glioblastoma tumors by MRI-guided CED of magnetic nanoparticles may provide more effective treatment of these devastating brain tumors. We recognize that the rodent model may not be the ideal animal model to study CED; however, our studies provide a proof-of-principle concept for future CED studies using other cancer nanotechnology agents.

In conclusion, the preclinical use of IONPs conjugated to a glioblastoma-specific antibody may form the basis of a future clinical trial of image-guided CED of magnetic nanoparticles for patients with glioblastoma tumors.

Disclosure of Potential Conflicts of Interest

No potential conflicts of interest were disclosed.

Grant Support

NIH grant NS053454 (C.G. Hadjipanayis), NIH Center for Cancer Nanotechnology in Excellence Program grant 54 CA119338-01 (H. Mao), NIH grant P50CA128301-01A10003 (H. Mao and C.G. Hadjipanayis), EmTech Bio, Inc. (H. Mao), Southeastern Brain Tumor Foundation (C.G. Hadjipanayis), the Georgia Cancer Coalition, Distinguished Cancer Clinicians and Scientists Program (C.G. Hadjipanayis), and the Dana Foundation (C.G. Hadjipanayis).

The costs of publication of this article were defrayed in part by the payment of page charges. This article must therefore be hereby marked *advertisement* in accordance with 18 U.S.C. Section 1734 solely to indicate this fact.

Received 03/23/2010; revised 05/11/2010; accepted 05/25/2010; published OnlineFirst 07/20/2010.

References

1. Van Meir EG, Hadjipanayis CG, Norden AD, Shu HK, Wen PY, Olson JJ. Exciting new advances in neuro-oncology: the avenue to a cure for malignant glioma. CA Cancer J Clin 2010;60:166–93.
2. Hadjipanayis CG, Van Meir EG. Brain cancer propagating cells: biology, genetics and targeted therapies. Trends Mol Med 2009;15: 519–30.
3. Singh SK, Hawkins C, Clarke ID, et al. Identification of human brain tumour initiating cells. Nature 2004;432:396–401.
4. Nishikawa R, Ji XD, Harmon RC, et al. A mutant epidermal growth factor receptor common in human glioma confers enhanced tumorigenicity. Proc Natl Acad Sci U S A 1994;91:7727–31.
5. Li B, Yuan M, Kim IA, Chang CM, Bernhard EJ, Shu HK. Mutant epidermal growth factor receptor displays increased signaling through the phosphatidylinositol-3 kinase/AKT pathway and promotes radioresistance in cells of astrocytic origin. Oncogene 2004; 23:4594–602.
6. Libermann TA, Nusbaum HR, Razon N, et al. Amplification, enhanced expression and possible rearrangement of EGF receptor gene in primary human brain tumours of glial origin. Nature 1985;313:144–7.
7. Bigner SH, Humphrey PA, Wong AJ, et al. Characterization of the epidermal growth factor receptor in human glioma cell lines and xenografts. Cancer Res 1990;50:8017–22.
8. Humphrey PA, Wong AJ, Vogelstein B, et al. Anti-synthetic peptide antibody reacting at the fusion junction of deletion-mutant epidermal growth factor receptors in human glioblastoma. Proc Natl Acad Sci U S A 1990;87:4207–11.
9. Wikstrand CJ, Hale LP, Batra SK, et al. Monoclonal antibodies against EGFRvIII are tumor specific and react with breast and lung carcinomas and malignant gliomas. Cancer Res 1995;55:3140–8.
10. Sampson JH, Archer GE, Mitchell DA, Heimberger AB, Bigner DD. Tumor-specific immunotherapy targeting the EGFRvIII mutation in patients with malignant glioma. Semin Immunol 2008;20:267–75.
11. Bulte JW, Kraitchman DL. Iron oxide MR contrast agents for molecular and cellular imaging. NMR Biomed 2004;17:484–99.
12. Moore A, Weissleder R, Bogdanov A, Jr. Uptake of dextran-coated monocrystalline iron oxides in tumor cells and macrophages. J Magn Reson Imaging 1997;7:1140–5.
13. Maier-Hauff K, Rothe R, Scholz R, et al. Intracranial thermotherapy using magnetic nanoparticles combined with external beam radiotherapy: results of a feasibility study on patients with glioblastoma multiforme. J Neurooncol 2007;81:53–60.
14. Nasongkla N, Bey E, Ren J, et al. Multifunctional polymeric micelles as cancer-targeted, MRI-ultrasensitive drug delivery systems. Nano Lett 2006;6:2427–30.
15. Chertok B, David AE, Huang Y, Yang VC. Glioma selectivity of magnetically targeted nanoparticles: a role of abnormal tumor hydrodynamics. J Control Release 2007;122:315–23.
16. Yang L, Peng XH, Wang YA, et al. Receptor-targeted nanoparticles for *in vivo* imaging of breast cancer. Clin Cancer Res 2009; 15:4722–32.
17. Hadjipanayis CG, Bonder MJ, Balakrishnan S, Wang X, Mao H, Hadjipanayis GC. Metallic iron nanoparticles for MRI contrast enhancement and local hyperthermia. Small 2008;4:1925–9.
18. Neuwelt EA, Varallyay P, Bago AG, Muldoon LL, Nesbit G, Nixon R. Imaging of iron oxide nanoparticles by MR and light microscopy in patients with malignant brain tumours. Neuropathol Appl Neurobiol 2004;30:456–71.
19. Shapiro EM, Skrtic S, Sharer K, Hill JM, Dunbar CE, Koretsky AP. MRI detection of single particles for cellular imaging. Proc Natl Acad Sci U S A 2004;101:10901–6.
20. Lee JH, Huh YM, Jun YW, et al. Artificially engineered magnetic nanoparticles for ultra-sensitive molecular imaging. Nat Med 2007; 13:95–9.
21. Hilger I, Kiebling A, Romanus E, et al. Magnetic nanoparticles for selective heating of magnetically labelled cells in culture: preliminary investigation. Nanotechnology 2004;15:1027–32.
22. Jordan A, Scholz R, Maier-Hauff K, et al. The effect of thermotherapy using magnetic nanoparticles on rat malignant glioma. J Neurooncol 2006;78:7–14.
23. Ohno T, Wakabayashi T, Takemura A, et al. Effective solitary hyperthermia treatment of malignant glioma using stick type CMC-magnetite. *In vivo* study. J Neurooncol 2002;56:233–9.
24. Koo YE, Reddy GR, Bhojani M, et al. Brain cancer diagnosis and therapy with nanoplatforms. Adv Drug Deliv Rev 2006;58: 1556–77.
25. Reddy GR, Bhojani MS, McConville P, et al. Vascular targeted nanoparticles for imaging and treatment of brain tumors. Clin Cancer Res 2006;12:6677–86.
26. Bobo RH, Laske DW, Akbasak A, Morrison PF, Dedrick RL, Oldfield EH. Convection-enhanced delivery of macromolecules in the brain. Proc Natl Acad Sci U S A 1994;91:2076–80.
27. Hadjipanayis CG, Fellows-Mayle W, Deluca NA. Therapeutic efficacy of a herpes simplex virus in combination with radiation or temozolomide for intracranial glioblastoma after convection-enhanced delivery. Mol Ther 2008;16:1783–8.
28. Song JH, Bellail A, Tse MC, Yong VW, Hao C. Human astrocytes are resistant to Fas ligand and tumor necrosis factor-related apoptosis-inducing ligand-induced apoptosis. J Neurosci 2006;26: 3299–308.
29. Gao X, Cui Y, Levenson RM, Chung LW, Nie S. *In vivo* cancer targeting and imaging with semiconductor quantum dots. Nat Biotechnol 2004;22:969–76.
30. Chakravarti A, Dicker A, Mehta M. The contribution of epidermal growth factor receptor (EGFR) signaling pathway to radioresistance in human gliomas: a review of preclinical and correlative clinical data. Int J Radiat Oncol Biol Phys 2004;58:927–31.
31. Mendelsohn J, Baselga J. The EGF receptor family as targets for cancer therapy. Oncogene 2000;19:6550–65.
32. Kunwar S, Prados MD, Chang SM, et al. Direct intracerebral delivery of cintredekin besudotox (IL13-38QQR) in recurrent malignant glioma: a report by the Cintredekin Besudotox Intraparenchymal Study Group. J Clin Oncol 2007;25:837–44.
33. Sampson JH, Akabani G, Archer GE, et al. Intracerebral infusion of an EGFR-targeted toxin in recurrent malignant brain tumors. Neuro Oncol 2008;10:320–9.
34. Sun C, Veiseh O, Gunn J, et al. *In vivo* MRI detection of gliomas by chlorotoxin-conjugated superparamagnetic nanoprobes. Small 2008;4:372–9.
35. Neuwelt EA, Varallyay CG, Manninger S, et al. The potential of ferumoxytol nanoparticle magnetic resonance imaging, perfusion, and angiography in central nervous system malignancy: a pilot study. Neurosurgery 2007;60:601–11, discussion 11–2.
36. Veiseh O, Sun C, Gunn J, et al. Optical and MRI multifunctional nanoprobe for targeting gliomas. Nano Lett 2005;5:1003–8.
37. Veiseh O, Sun C, Fang C, et al. Specific targeting of brain tumors with an optical/magnetic resonance imaging nanoprobe across the blood-brain barrier. Cancer Res 2009;69:6200–7.
38. Orringer DA, Koo YE, Chen T, Kopelman R, Sagher O, Philbert MA. Small solutions for big problems: the application of nanoparticles to brain tumor diagnosis and therapy. Clin Pharmacol Ther 2009;85:531–4.
39. Weinstein JS, Varallyay CG, Dosa E, et al. Superparamagnetic iron oxide nanoparticles: diagnostic magnetic resonance imaging and potential therapeutic applications in neurooncology and central nervous system inflammatory pathologies, a review. J Cereb Blood Flow Metab 2010;30:15–35.
40. Morrison PF, Laske DW, Bobo H, Oldfield EH, Dedrick RL. High-flow microinfusion: tissue penetration and pharmacodynamics. Am J Physiol 1994;266:R292–305.
41. Voges J, Reszka R, Gossmann A, et al. Imaging-guided convection-enhanced delivery and gene therapy of glioblastoma. Ann Neurol 2003;54:479–87.
42. Croteau D, Walbridge S, Morrison PF, et al. Real-time *in vivo* imaging of the convective distribution of a low-molecular-weight tracer. J Neurosurg 2005;102:90–7.
43. Sampson JH, Akabani G, Friedman AH, et al. Comparison of intratumoral bolus injection and convection-enhanced delivery of radiolabeled antitenascin monoclonal antibodies. Neurosurg Focus 2006; 20:E14.

44. Dickinson PJ, LeCouteur RA, Higgins RJ, et al. Canine model of convection-enhanced delivery of liposomes containing CPT-11 monitored with real-time magnetic resonance imaging: laboratory investigation. J Neurosurg 2008;108:989–98.
45. Perlstein B, Ram Z, Daniels D, et al. Convection-enhanced delivery of maghemite nanoparticles: increased efficacy and MRI monitoring. Neuro Oncol 2008;10:153–61.
46. Lustig R. Long term responses with cetuximab therapy in glioblastoma multiforme. Cancer Biol Ther 2006;5:1242–3.
47. Mellinghoff IK, Wang MY, Vivanco I, et al. Molecular determinants of the response of glioblastomas to EGFR kinase inhibitors. N Engl J Med 2005;353:2012–24.
48. Neyns B, Sadones J, Joosens E, et al. Stratified phase II trial of cetuximab in patients with recurrent high-grade glioma. Ann Oncol 2009;20:1596–603.
49. Balyasnikova IV, Ferguson SD, Sengupta S, Han Y, Lesniak MS. Mesenchymal stem cells modified with a single-chain antibody against EGFRvIII successfully inhibit the growth of human xenograft malignant glioma. PLoS One 2010;5:e9750.
50. Sampson JH, Crotty LE, Lee S, et al. Unarmed, tumor-specific monoclonal antibody effectively treats brain tumors. Proc Natl Acad Sci U S A 2000;97:7503–8.
51. Mishima K, Johns TG, Luwor RB, et al. Growth suppression of intracranial xenografted glioblastomas overexpressing mutant epidermal growth factor receptors by systemic administration of monoclonal antibody (mAb) 806, a novel monoclonal antibody directed to the receptor. Cancer Res 2001;61:5349–54.
52. Patel D, Lahiji A, Patel S, et al. Monoclonal antibody cetuximab binds to and down-regulates constitutively activated epidermal growth factor receptor vIII on the cell surface. Anticancer Res 2007;27:3355–66.
53. Moore A, Marecos E, Bogdanov A, Jr., Weissleder R. Tumoral distribution of long-circulating dextran-coated iron oxide nanoparticles in a rodent model. Radiology 2000;214:568–74.
54. Zimmer C, Weissleder R, Poss K, Bogdanova A, Wright SC, Jr., Enochs WS. MR imaging of phagocytosis in experimental gliomas. Radiology 1995;197:533–8.
55. Villanueva A, Canete M, Roca AG, et al. The influence of surface functionalization on the enhanced internalization of magnetic nanoparticles in cancer cells. Nanotechnology 2009;20:115103.